SI MATERIALS AND METHODS

Darlingtonia natural history

The digestive communities contained within the leaves of carnivorous pitcher plants (families Nepenthaceae, Cephalotaceae, and Sarraceniaceae) are particularly well suited for the study of microbial succession and ecosystem development. These plants have adapted to grow on nutrient-poor substrates by evolving the ability to lure, capture, and digest invertebrate prey using fluid-filled leaves. The captured prey form the base of a simple aquatic food web reliant on proteolytic enzymes produced by the plant and its commensal bacteria, which function to mineralize growth-limiting nutrients (primarily nitrogen and phosphorous) for uptake by the host leaf (Hepburn *et al.*, 1927; Juniper *et al.*, 1989; Butler *et al.*, 2008).

The pitcher plant *Darlingtonia californica* (Sarraceniaceae) is native to California and Oregon, USA, where it grows in spring-fed wet meadows on or near serpentine formations. Each plant produces up to 15 pitcher leaves during its June-October growing season with the first leaf being the year's largest (up to 0.75 m). Leaves begin to senesce after their first growing season but persist for up to 1.5 years. The pitcher leaf completes its vertical growth prior to opening its trapping orifice and its interior chamber is sterile until this point (D. W. Armitage, *unpubl. data*). Compared to other members of Sarraceniaceae, *Darlingtonia* has a unique downward-oriented trapping orifice that minimizes passive dispersal into pitchers and prevents flooding. Instead, the leaf actively secretes water into its chamber in response to prey capture. Two arthropods are found in nearly every pitcher leaf days after opening: obligate histiostomatid mite *Sarraceniopus darlingtoniae,* which feeds on bacterial biofilms*,* and larvae of the obligate midge *Metriocnemus edwardsi,* which feeds directly on the captured prey. Detritivorous bacteria, as well as bacterivorous flagellates, ciliates, and rotifers, are carried into pitchers on or inside of captured prey. The unique downward-facing

orifice of *Darlingtonia* pitchers makes passive airborne or waterborne dispersal unlikely. The majority of prey capture by *Darlingtonia* typically occurs during a leaf's first two months, after which it ceases nectar production. Prey composition varies strongly between leaves of the same age, but consists primarily of Hymenoptera, Coleoptera, and Diptera (Armitage, 2016). Like its close relative *Sarracenia purpurea*, *Darlingtonia* is believed to primarily rely on the actions of its food web for digestion (Hepburn *et al.*, 1927; Lindquist, 1975; Naeem, 1988; Gallie and Chang, 1997; Cochran-Stafira and von Ende, 1998; Mouquet *et al.*, 2008), as opposed to digestive enzymes. In particular, *S. purpurea* was found to rely almost entirely on the bacteria (as opposed to mites and insect larvae) for nitrogen acquisition (Butler *et al.*, 2008). And although fungi are present in leaf tissues, they are not abundant in pitcher fluid (*pers. obs*) and do not participate heavily in prey decomposition, compared to bacteria and midge larvae (Lindquist, 1975; Mayer, 2005).

Stable isotope labeling of plants in the field

I conducted the study during June-Nov 2013 in a large population of *Darlingtonia californica* pitcher plants growing near the Butterfly Valley Botanical Area in Plumas National Forest (Plumas Co., CA) and repeated the study in 2014 in a nearby population in the same forest. Both populations occur in permanently saturated, spring-fed montane fens separated by approximately 2 km and contain over 3 000 individual plants. *Darlingtonia* plants in both populations co-occurred with *Rhododendron occidentale*, *Carex spp.*, and grew on thick mats of *Sphagnum* moss. Switching populations between years was necessary to mitigate carryover contamination effects from the previous year's isotopic enrichments. Each year, at the beginning of the growing season in early June, I identified and tagged 50 pitcher leaves of equivalent developmental stage on different plants. These leaves represented a single cohort of each plant's first (and largest) pitcher leaves. In order to control for the

underground transport of nitrogen between study leaves, I selected leaves from individual clusters of rosettes such that were derived from different, unconnected genets. In addition, study leaves were never located on neighboring rosette clusters, and were always separated by at least 5 m. I monitored these leaves daily to determine the date at which each leaf's trapping orifice opened. All study leaves opened and began trapping insects on the same day.

To measure rates of decomposition and nitrogen cycling by the pitchers' aquatic food webs, I fed to each pitcher one gelatin capsule filled with 20 sterile, ^{15}N-enriched fruit flies (*Drosophila melanogaster*). I used an existing protocol to create the isotope-labeled flies (Gouw *et al.*, 2011). Briefly, I let adult flies mate and lay eggs in unlabeled yeast paste. Eggs were harvested by rinsing the paste over 10 µm mesh and briefly washed in 70% EtOH and sterile dH_2O. These eggs were spread onto a sterile Whatman #1 filter and placed into a box containing a sterile cotton sheet soaked in a larval fly diet consisting of 70 mL sterile dH_2O, 37.5 µl propionic acid, 240 µl phosphoric acid, 840 µl 10% w/v tegosept, 3 µg ampicillin, 9 g sucrose, and 9 g (dry weight) ^{15}N-labeled yeast. Isotope-labeling of yeast was achieved by culturing yeast in 1.7 g/l YNB without amino acids and ammonium sulfate (Difco^{TM}) with 20 g/L sucrose and 5 g/l >99 atom% ^{15}N-labeled ammonium sulfate (Cambridge Isotope Laboratories). Yeast cultures were shaken for 24 hours at 30° C. The culture was divided into 250 ml Nalgene tubes and centrifuged at 2,400 × *g* for 20 min at 4° C. The supernatant was removed and the pellets were re-suspended in 10 mL sterile phosphate buffer (PBS) and pooled into sterile 50 mL centrifuge tubes until I obtained the equivalent of 9 g dry weight. Once the eggs were added, the fly box was covered with mesh and placed in a dark growth chamber at 30° C and 95% humidity. Adult flies were collected daily and stored at -20° C. Once 2000 flies had been obtained, they were dried for 3 days at 60° C, grouped into lots of 20 individuals, weighed on a microbalance, autoclaved, and stored in 0.2 ml PCR tubes at -20° C. Four flies were sent to the UC Davis Isotope Facility for gas chromatography - isotope

ratio mass spectrometry (GC-IRMS). These flies were enriched to 82 atom% (± 1.9% SEM) ^{15}N.

On the day the pitcher leaves first opened, I randomly selected five leaves to receive 20 ^{15}N-enriched fruit flies via a gel cap, which quickly dissolved. After 11 days, I returned to the site and collected the five ^{15}N-labeled pitcher leaves. These leaves were placed in sterile icewater and immediately transported to the lab. On the same day, 5 more pitchers were randomly fed gel caps containing ^{15}N-labeled flies. This process was repeated every 11 days up to day 88 (mid-September), and again on day 166 (late November 2014) and on day 365 (June 2014, 2015) with 10 tagged leaves from the previous year. This timeframe was chosen to minimize the effects of plant dormancy, temperature fluctuations, and prey availability on the measured leaf characteristics.

Microscopy of pitcher contents

Immediately after returning to the lab, I quantified all components of each pitcher leaf's food web. I removed the upper 2/3 of the leaf using a pair of sterilized scissors. The lower portion of the leaf, including the digestive zone and fluid, was placed into a sterile 50 ml falcon tube on ice. I dissected the upper portion of the leaf down its midrib and pinned it on an insect pinning block. I used a dissecting microscope to count and identify all living arthropods on the abaxial surface (Nielsen, 1990). Next, I used a pipette to remove all liquid from the lower portion of each pitcher leaf and I recorded the volume of fluid each leaf contained (mean = 2.7 ml, sd = 2.7 ml, min = 0.1 ml, max = 10 ml). When insufficient raw fluid was able to be obtained from a leaf, I added to the chamber 2 ml of sterile phosphate buffer, briefly agitated it using a pipette, and removed the fluid after 20 minutes. Measurements taken from these samples were corrected for the added buffer's dilution effects. This fluid was placed in a sterile 15 ml flask on ice. I dissected the bottom portion of the leaf and emptied its contents

101 onto a petri dish. I counted all mite and midge larvae in the dish and then searched for all
102 fruit fly remains and repeated this process on the sidewalls of the digestive chamber. Then,
103 after thoroughly rinsing each leaf of any residual arthropod material in dH_2O, I dried each
104 dissected leaf in a drying oven for 3 days at 60° C. I did the same for each pitcher's prey
105 items after having removed the midge larvae and any visible fruit flies. I used the condition
106 of the recovered fruit flies to rate the extent of prey decomposition on a 5-point ordinal scale.
107 If all flies were recovered intact with no visible damage (e.g., missing limbs, abdominal
108 segments.), the pitcher was scored a zero. If no flies were recoverable and head-capsules
109 were found, then the pitcher was scored as five. Intermediate values depended on both the
110 number of flies recovered and the extent of their decomposition.
111 I quantified and identified all microinvertebrates and protists using Sedgwick Rafter
112 (1 ml) and Palmer (0.1 ml) counting cells. I filled each counting cell with a vortexed aliquot
113 of pitcher fluid containing either Proto-Slo (Carolina Biological, Inc.) or 3% Lugol's iodine
114 solution (Sherr and Sherr, 1993). Individual organisms were counted in random circular
115 fields until at least 200 had been counted and estimated their abundances using the formula
116 $d = n \div F \cdot A_c \div A_f \div V,$ where d is the estimated density of individuals per unit volume, n
117 is the total number of individuals counted across all fields, F is the total number of fields
118 counted, A_c and A_f are the areas (μm^2) encompassed by the full chamber and the ocular field,
119 respectively, and V is the total dilution-corrected volume (ml) of fluid in the chamber.
120 If fewer than 200 individuals of a particular taxon could be found in the chamber, the total
121 number of individuals in the chamber was counted. I attempted to identify all micro-
122 invertebrates and protists using dichotomous keys (Lee *et al.*, 2000) and previous accounts of
123 pitcher plant-associates (Laird, 1969).
124 Epifluorescence microscopy was used to quantify bacterial and viral abundances in
125 the fluid of N-labeled pitchers (Patel *et al.*, 2007). I created serial dilutions of pitcher fluid in

0.02 μm-filtered phosphate buffer and added to them sterile sodium pyrophosphate solution to 5 mM. This step causes the elution of particle-bound bacteria and viruses and results in a lower CV between samples (Danovaro *et al.*, 2001). These samples were briefly vortexed and 0.5 mL aliquots of varying dilutions (typically 10^3 for bacteria and 10^4 for viruses) were vacuum-filtered onto 0.02 μm Anodisc 25 filters (Whatman, Inc.). Filters were made in triplicate for each pitcher sample and dilution. After drying, I stained filters with 100 μl 0.5× SYBR-gold nucleic acid stain for 15 minutes in the dark. This stain binds to DNA and produces a green fluorescent signal under blue excitation, and is used to enumerate bacteria, archaea, and virus-like particles (VLPs) (Patel *et al.*, 2007). After a second round of drying, the filters were mounted on glass microscope slides using 0.02 μm-filtered glycerol-based anti-fade solution. To avoid photobleaching of slides during counting, I photographed random fields of each filter at 1 000× magnification under blue excitation and counted them later. VLP and bacterial/archaeal abundances were estimated following the protocol of (Patel *et al.*, 2007). All slides were made less than 8 hours after collection from the field and less than 1 hour after pitcher fluid was removed from the plant.

Pitcher community carbon mineralization

I estimated the each N-labeled pitcher leaf community's potential rate of carbon mineralization using the MicroResp™ respirometry system following the manufacturer's protocol (Campbell *et al.*, 2003). I added 100 μl of 20 μm-filtered pitcher fluid to 900 μl sterile phosphate buffer in a microcentrifuge tube and centrifuged the mixture at 10 000 × *g* for 5 minutes. I removed the supernatant, added in clean buffer, and resuspended the pellet. This process was repeated twice to wash bacterial communities of any residual medium, and the final bacterial community was starved for 2 hours prior to inoculation into the respirometry chambers. I added 50 μl of starved, dilute pitcher fluid into 750 μl medium

151 comprised of M9 salt solution (NH_4Cl 1 g l^{-1}, Na_2HPO_4 6 g l^{-1}, KH_2PO_4 3 g l^{-1}, NaCl 0.5 g l^{-1},
152 pH 6.0) and 3 g l^{-1} powder from freeze-dried crickets that had been ground and autoclaved. I
153 inoculated each sample into a sterile 1.2 mL 96-well plate. Onto this plate I clamped a
154 standard 96-well plate containing a redox dye set in purified agar. Inoculated MicroResp
155 containers were placed in an incubator for three days at 25° C. Rates of CO_2-C evolution
156 over time were be estimated by taking the absorbances of dyed agar wells at 490 nm on a
157 Molecular Devices ^{TM} Emax microplate reader at 490 nm. Each community's respiration was
158 averaged over six independent replicates. These rates of CO_2 respiration reflect the potential
159 respiration rates of each pitcher's bacterial community in a common habitat, which allowed
160 me to compare each community's relative performances without the confounding effects of
161 pitcher chemistry and nutrient availability.
162 I used the Biolog GN2 microplate assay (Biolog Inc., Hayward, CA) to measure the
163 carbon substrate utilization patterns of the microbial communities from an independent
164 collection of 11, 55, and 365 day-old pitchers (10 from each age, 5 per year). Each well of
165 the GN2 microplate contained a different carbon substrate (95 total) and a dye that changes
166 color when reduced by NADP(H). A color change in a well indicated that at least one taxon
167 in the inoculum was capable of growth on the particular C-substrate. Plates were inoculated
168 using the same dilute, filtered, starved communities described above, and incubated for 3
169 days at 25° C. Each community was run in triplicate, and only wells that showed a color
170 change in all three replicates were scored as positive for metabolism. I used a negative
171 binomial generalized linear model to determine whether the number of metabolized
172 substrates differed among age classes and ran a chi-square likelihood ratio test to compare
173 the fit of the parameterized model to that of an intercept-only null.
174
175 **Measuring pitcher nitrogen uptake efficiency**

Once the fluid had been collected and prey removed from each pitcher, I thoroughly washed the leaf tissue in DI water to remove as much remaining arthropod material as possible. Each leaf was then dried for 3 days at 60° C, weighed, and ground using a Wiley Mill. I removed a subsample of this tissue and ground it to a fine powder using a bead beater. These powdered samples were weighed, packaged in tin capsules, and sent to the UC Davis Stable Isotope Facility (Davis, CA) for gas chromatography-isotope ratio mass spectrometry (GC-IRMS). I estimated the nitrogen uptake efficiency (N_{eff}) of each pitcher leaf using the formula

$$N_{eff} = 100 \cdot \frac{[\mathrm{N}_{leaf} \cdot (\mathrm{at\%}^{15}\mathrm{N}_{leaf} - \mathrm{at\%}^{15}\mathrm{N}_{ref})]}{(\mu\mathrm{g}_{fly} \cdot \mathrm{N}_{fly} \cdot \mathrm{at\%}^{15}\mathrm{N}_{fly})} \quad (1)$$

where N_i is the total mass of nitrogen (μg) in leaf or fly tissue, at%$^{15}N_i$ are the atom percent measurements of ^{15}N in either leaf tissue, fly tissue, or atmospheric reference samples, and μg_{fly} is the total mass of flies added to the pitcher leaf. This value is an estimate of the total fraction of nitrogen from the added flies that was found in the host pitcher's tissue after 11 days (Butler *et al.*, 2008).

Amplicon sequencing of bacterial communities

I used the MoBio Powersoil DNA Extraction Kit (MoBio Laboratories, Carlsbad, CA) to extract community DNA from 700 μl aliquots of 20 μm pitcher fluid filtrate. After NanoDrop quantification, all samples were stored at -80° C. A control extraction from each Powersoil kit was also performed to check for contamination. Once all samples and blanks were collected, they were sent for sequencing at the Argonne National Laboratory Core Sequencing Facility (Lemont, IL) using Earth Microbiome Project (EMP) protocols (Caporaso *et al.*, 2012). Briefly, this involved PCR amplification of the 16S ribosomal RNA region, including EMP adapters, multiplex barcodes, linker sequences, and primer sequences 515F (5'– AATGATACGGCGACCACCGAGATCTACAC XXXXXXXXXXXX TATGGTAATT GT GTGYCAGCMGCCGCGGTAA – 3') and 806R (5'–

CAAGCAGAAGACGGCATACGAGAT AGTCAGTCAG CC
GGACTACNVGGGTWTCTAAT – 3'). The field containing X's represents a unique 12-bp barcode to distinguish pooled samples. Thermocycling followed the EMP protocol: a denaturing step at 94° C for 3 minutes, amplification for 35 cycles at 94° C for 45 seconds, 50° C for 60 seconds, 72° C for 60 seconds, and a final extension at 72° C for 10 minutes (Caporaso *et al.*, 2012). Paired-end 2x150 bp sequencing was carried out on an Illumina MiSeq. Sequences were deposited in the public MG-RAST (http://metagenomics.anl.gov/) server under project mgp14344.

I demultiplexed pooled 16S reads using the QIIME platform (quality parameters q = 20 and p = 0.9) (Caporaso *et al.*, 2010b) and assembled paired ends using SeqPrep (St. John). Next, I removed chimeric sequences using both reference-based (using the RDP database) and *de novo* UCHIME (Edgar *et al.*, 2011; Cole *et al.*, 2014). I clustered reads into operational taxonomic units (OTUs) at 97% sequence similarity using an open-reference approach (Rideout *et al.*, 2014). This involved first clustering sequences to representative OTUs in the Greengenes 13.8 database (DeSantis *et al.*, 2006) using SortMeRNA (Kopylova *et al.*, 2012), and then performing *de novo* clustering on the remaining sequences using SUMACLUST (Mercier *et al.*, 2016). Sequences were then aligned using PyNAST (Caporaso *et al.*, 2010a), assigned to taxonomy using SortMeRNA and the Greengenes database (Bokulich *et al.*, 2015), and used to build a phylogenetic tree with FastTree 2.1 (Price *et al.*, 2010). I removed singletons, OTUs shared with kit blanks, and low-confidence OTUs (those representing less than 0.1% of the sample's total reads). To account for differences in sequencing depths among samples, I normalized OTU tables using library size factor (LSF) scaling implemented in the *DESeq2* R package (Love *et al.*, 2014). This pipeline is illustrated in figure S1.

Statistical analyses

I combined sample metadata (e.g., pitcher N uptake efficiency, bacterial abundance, pitcher age), phylogenetic data, and OTU tables using the *PhyloSeq* package in R (McMurdie and Holmes, 2013; R Development Core Team, 2015). Exploratory analyses did not reveal any systematic differences between the two study years, so data were pooled for all analyses unless otherwise indicated. Bacterial alpha diversity was measured using Shannon's diversity index (H') and Faith's (Faith, 1992) phylogenetic diversity. Temporal differences in bacterial diversity, bacterivore richness, and the abundances of each major food web compartment (detritus, viruses, bacteria, *Polytomella,* mites and midges) were analyzed using ANOVA. I conducted post-hoc analyses using Tukey's range test. When necessary, data were log-transformed for variance stabilization. No model residuals showed heteroskedasticity or temporal autocorrelation.

Using normalized OTU tables, I calculated Jensen-Shannon distance (Marcon *et al.*, 2014), and weighted and unweighted UniFrac metrics (Lozupone *et al.*, 2011) to characterize the distances between pitcher samples. Using the *vegan* package in R (Oksanen *et al.*, 2015), I plotted these samples on their primary principal coordinates axes (PCoA). Similarly, I used PCoA to visualize temporal differences in Biolog plate substrate utilization measured using Jaccard's dissimilarity. Eigenvalues, which were always greater than zero, were used to estimate the percentage of variance explained by the first two principal coordinates. I used permutational analysis of variance (PERMANOVA) with the *adonis* function in R (Anderson, 2001) to assess whether intra-age dissimilarities were significantly less than inter-age dissimilarities for each data table (bacteria, bacterivores, C-substrates). To determine whether bacterial communities converged or diverged over time, I compared average pairwise community dissimilarities among pitcher age classes using ANOVA. I used two

different dissimilarity measures: unweighted UniFrac (phylogeny-based) and Jensen-Shannon distance (OTU-based).

I modeled LSF-normalized OTU counts using a negative binomial generalized linear model (GLM). For an OTU *i* in sample *j*, OTU counts, K_{ij}, were modeled as

$$K_{ij} \sim NB(\text{mean} = \mu_{ij}, \text{dispersion} = \alpha_{ij}) \quad (2)$$

$$\mu_{ij} = s_{ij} q_{ij} \quad (3)$$

$$\log_2 q_{ij} = \beta_i^0 + \beta_i^{\text{A}} x_i^{\text{A}} \quad (4)$$

where x_i^{A} is the pitcher sample's age category, β_i^{A} are parameters describing the log-fold change of an OTU in each age class, and s_{ij} is the OTU and age-specific normalization factor (for further details, see (Love *et al.*, 2014). Modeling OTU turnover using their $\log_2$-fold changes in abundance circumvents problems caused by heteroscedastic raw count data. Models were fit using empirical Bayes and OTUs experiencing significant $\log_2$-fold change among time points were identified using multiple testing-corrected Wald *p*-values.

I defined the 'successional microbiome' as the subset of OTUs experiencing a statistically significant ($\alpha = 0.01$) $\geq$ 8-fold change in abundance between any two leaf age classes. I used these OTUs to build an abundance-weighted heat map and sorted OTUs along the y-axis based on the pitcher age group in which they first appear. I assessed the predictive accuracy of this subset of OTUs by training a random forest (RF) classifier (Breiman, 2001) (10000 trees total) on the successional OTU counts from 2013 and using the resulting model to predict the ages of 2014 samples. The predictive model was fit to minimize the error rate between observed and OOB data. Model accuracy was evaluated using the coefficient of determination (R^2) for predicted vs. observed points along a 1:1 line. I additionally trained the RF classifier on both years' data and used 10-fold cross-validation to assess the overall model's accuracy.

Estimating functional gene turnover

For the subset of closed-reference OTUs detected in my samples, I used the PICRUSt (Phylogenetic Investigation of Communities by Reconstruction of Unobserved States) software (Langille *et al.*, 2013) to predict each OTU's rRNA copy number and functional gene content. The PICRUSt algorithm identifies the closest relatives of each OTU for which annotated genomes are available and performs ancestral state reconstructions to estimate its gene contents. The accuracy of this method depends on the evolutionary distances between an OTU and its nearest reference genome (measured by the 'nearest sequenced taxon index', NSTI), but is generally greater than 75% for samples falling in the range of NSTI values in my samples (0.071 ± 0.01 SEM) and can be greater than 90% for certain orthologous gene categories (e.g., amino acid and carbohydrate metabolism) (Langille *et al.*, 2013). I used the Kyoto Encyclopedia of Genes and Genomes (KEGG) database for all gene annotations (Kanehisa *et al.*, 2016). To account for variable sequencing depth among samples, PICRUSt predictions were made using an LSF-normalized OTU table.

I estimated the mean weighted rRNA copy number, C_{ij}, for each sample using the method of (Nemergut *et al.*, 2015): $C_{ij} = \sum p_{ij} c_i$, where p_{ij} is the relative abundance of OTU i in sample j and c_i is the PICRUSt-estimated rRNA copy number of OTU i. ANOVA was used to determine whether predicted rRNA copy numbers changed over time. Next, I ordinated pitcher samples based on their level 3 KEGG pathway relative abundances using principal components analysis (PCA). In addition, samples were hierarchically clustered based on Euclidean distances among their level 3 KEGG pathways using Ward's method (Ward, 1963). I used ANOVA to identify KEGG pathways that differed in relative abundances through time. To remove potentially spurious results, I filtered KEGG pathways by p-value ($p \leq 0.01$) and effect size ($\eta^2 \geq 0.26$). All p-values were first corrected for multiple testing using the Benjamini-Hochberg procedure. In addition to KEGG pathways, I plotted

300 the raw abundances of individual KEGG Ortholog genes over time, focusing primarily on
301 enzymes involved in the ammonification, nitrate reduction, denitrification, and nitrogen
302 fixation pathways. All tests were run using STAMP 2.0 (Parks and Beiko, 2010) and R.
303 Because data generated by PICRUSt software are predictions, I did not subject any of these
304 data to formal hypothesis tests and instead let them stand as hypotheses to be falsified using
305 direct metagenomic or metatranscriptomic sequences.
306

307 **REFERENCES**

308 Anderson MJ. (2001). A new method for non-parametric multivariate analysis of variance.
309 *Austral Ecol* **26**: 32–46.

310 Armitage DW. (2016). The cobra's tongue: Rethinking the function of the 'fishtail
311 appendage' on the pitcher plant *Darlingtonia californica*. *Am J Bot* **103**: 780–785.

312 Bokulich N, Rideout JR, Kopylova E, Bolyen E, Patnode J, Ellett Z, *et al.* (2015). A
313 standardized, extensible framework for optimizing classification improves marker-gene
314 taxonomic assignments. *PeerJ Prepr* **3**: e1502.

315 Breiman L. (2001). Random forests. *Mach Learn* **45**: 5–32.

316 Butler JL, Gotelli NJ, Ellison AM. (2008). Linking the brown and green: nutrient
317 transformation and fate in the *Sarracenia* microecosystem. *Ecology* **89**: 898–904.

318 Campbell CD, Chapman SJ, Cameron CM, Davidson MS, Potts JM. (2003). A rapid
319 microtiter plate method to measure carbon dioxide evolved from carbon substrate
320 amendments so as to determine the physiological profiles of soil microbial communities by
321 using whole soil. *Appl Environ Microbiol* **69**: 3593–3599.

322 Caporaso JG, Bittinger K, Bushman FD, DeSantis TZ, Andersen GL, Knight R. (2010a).
323 PyNAST: a flexible tool for aligning sequences to a template alignment. *Bioinformatics* **26**:
324 266–267.

325 Caporaso JG, Kuczynski J, Stombaugh J, Bittinger K, Bushman FD, Costello EK, *et al.*
326 (2010b). QIIME allows analysis of high-throughput community sequencing data. *Nat*
327 *Methods* **7**: 335–336.

328 Caporaso JG, Lauber CL, Walters WA, Berg-Lyons D, Huntley J, Fierer N, *et al.* (2012).
329 Ultra-high-throughput microbial community analysis on the Illumina HiSeq and MiSeq
330 platforms. *ISME J* **6**: 1621–1624.

331 Cochran-Stafira DL, von Ende CN. (1998). Integrating bacteria into food webs: Studies with
332 *Sarracenia purpurea* inquilines. *Ecology* **79**: 880–898.

Cole JR, Wang Q, Fish JA, Chai B, McGarrell DM, Sun Y, *et al.* (2014). Ribosomal Database Project: data and tools for high throughput rRNA analysis. *Nucleic Acids Res* **42**: D633–D642.

Danovaro R, Dell'Anno A, Trucco A, Serresi M, Vanucci S. (2001). Determination of virus abundance in marine sediments. *Appl Environ Microbiol* **67**: 1384–1387.

DeSantis TZ, Hugenholtz P, Larsen N, Rojas M, Brodie EL, Keller K, *et al.* (2006). Greengenes, a chimera-checked 16S rRNA gene database and workbench compatible with ARB. *Appl Environ Microbiol* **72**: 5069–5072.

Edgar RC, Haas BJ, Clemente JC, Quince C, Knight R. (2011). UCHIME improves sensitivity and speed of chimera detection. *Bioinformatics* **27**: 2194–2200.

Faith DP. (1992). Conservation evaluation and phylogenetic diversity. *Biol Conserv* **61**: 1–10.

Gallie DR, Chang SC. (1997). Signal transduction in the carnivorous plant *Sarracenia purpurea*. Regulation of secretory hydrolase expression during development and in response to resources. *Plant Physiol* **115**: 1461–1471.

Gouw J, Tops BJ, Krijgsveld J. (2011). Metabolic labeling of model organisms using heavy nitrogen (^{15}N). In: Gevaert K, Vandekerckhove J (eds) Methods in Molecular Biology. *Gel-Free Proteomics*. Humana Press, pp 29–42.

Hepburn JS, Jones FM, John EQ. (1927). The biochemistry of the American pitcher plants: biochemical studies of the North American Sarraceniaceae. *Trans Wagner Free Inst Sci Phila* **1927**: 1–95.

Juniper BBE, Robins RJ, Joel DM. (1989). The Carnivorous Plants. Academic Press: London, UK; San Diego, CA.

Kanehisa M, Sato Y, Kawashima M, Furumichi M, Tanabe M. (2016). KEGG as a reference resource for gene and protein annotation. *Nucleic Acids Res* **44**: D457–D462.

Kopylova E, Noé L, Touzet H. (2012). SortMeRNA: fast and accurate filtering of ribosomal RNAs in metatranscriptomic data. *Bioinforma Oxf Engl* **28**: 3211–3217.

Laird DD. (1969). Pitcher plant, *Sarracenia purpurea* L., as an ecosystem. Master's Thesis, University of British Columbia: Vancouver, Canada.

Langille MGI, Zaneveld J, Caporaso JG, McDonald D, Knights D, Reyes JA, *et al.* (2013). Predictive functional profiling of microbial communities using 16S rRNA marker gene sequences. *Nat Biotechnol* **31**: 814–821.

Lee JJ, Leedale GF, Bradbury PC (eds). (2000). An illustrated guide to the protozoa. 2nd ed. Society of Protozoologists: Lawrence, KS.

Lindquist JA. (1975). Bacteriological and ecological observations on the northern pitcher plant, *Sarracenia purpurea* L. Ph.D dissertation, University of Wisconsin: Madison, WI, USA.

Love MI, Huber W, Anders S. (2014). Moderated estimation of fold change and dispersion for RNA-seq data with DESeq2. *Genome Biol* **15**: 1–21.

Lozupone C, Lladser ME, Knights D, Stombaugh J, Knight R. (2011). UniFrac: an effective distance metric for microbial community comparison. *ISME J* **5**: 169–172.

Marcon E, Scotti I, Hérault B, Rossi V, Lang G. (2014). Generalization of the partitioning of Shannon diversity. *PLOS ONE* **9**: e90289.

Mayer E. (2005). Karnivore Kesselfallenpflanzen – Untersuchungen zur Verdauung, Nährstoffaufnahme und Mikroflora. Diploma Thesis, University of Vienna: Vienna, Austria.

McMurdie PJ, Holmes S. (2013). phyloseq: an R package for reproducible interactive analysis and graphics of microbiome census data. *PLOS ONE* **8**: e61217.

Mercier C, Boyer F, Bonin A, Coissac E. (2016). SUMATRA and SUMACLUST: fast and exact comparison and clustering of sequences. https://git.metabarcoding.org/obitools/sumatra/wikis/home (Accessed March 23, 2016).

Mouquet N, Daufresne T, Gray SM, Miller TE. (2008). Modelling the relationship between a pitcher plant (*Sarracenia purpurea*) and its phytotelma community: mutualism or parasitism? *Funct Ecol* **22**: 728–737.

Naeem S. (1988). Resource heterogeneity fosters coexistence of a mite and a midge in pitcher plants. *Ecol Monogr* **58**: 215–227.

Nemergut DR, Knelman JE, Ferrenberg S, Bilinski T, Melbourne B, Jiang L, *et al.* (2015). Decreases in average bacterial community rRNA operon copy number during succession. *ISME J* **10**: 1147–1156.

Nielsen DW. (1990). Arthropod communities associated with *Darlingtonia californica*. *Ann Entomol Soc Am* **83**: 189–200.

Oksanen J, Blanchet FG, Kindt R, Legendre P, Minchin PR, O'Hara RB, *et al.* (2015). vegan: Community Ecology Package.

Parks DH, Beiko RG. (2010). Identifying biologically relevant differences between metagenomic communities. *Bioinformatics* **26**: 715–721.

Patel A, Noble RT, Steele JA, Schwalbach MS, Hewson I, Fuhrman JA. (2007). Virus and prokaryote enumeration from planktonic aquatic environments by epifluorescence microscopy with SYBR Green I. *Nat Protoc* **2**: 269–276.

Price MN, Dehal PS, Arkin AP. (2010). FastTree 2 – approximately maximum-likelihood trees for large alignments. *PLOS ONE* **5**: e9490.

R Development Core Team. (2015). R: A language and environment for statistical computing. R Foundation for Statistical Computing: Vienna, Austria.

Rideout JR, He Y, Navas-Molina JA, Walters WA, Ursell LK, Gibbons SM, *et al.* (2014). Subsampled open-reference clustering creates consistent, comprehensive OTU definitions and scales to billions of sequences. *PeerJ* **2**: e545.

Sherr EB, Sherr BF. (1993). Preservation and storage of samples for enumeration of heterotrophic protists. In: Kemp PF, Sherr BF, Sherr EB, Cole JJ (eds). *Handbook of methods in aquatic microbial ecology*. Lewis Publishers: London, UK, pp 207–212.

St. John J. SeqPrep. *GitHub*. https://github.com/jstjohn/SeqPrep (Accessed March 23, 2016).

Ward JH. (1963). Hierarchical grouping to optimize an objective function. *J Am Stat Assoc* **58**: 236–244.

Table S1. Permutational ANOVA (adonis) results for community similarity metrics. *P*-values ≤ 0.05 indicate samples are likely grouped by the covariate in question.

Response variable	Covariates	d.f.	Mean Squares	*F*-statistic	R^2	*p*-value
Jensen-Shannon distance	Year/Population	1	10.9	13.5	0.1	0.0001
	Community Age	9	2.7	3.3	0.23	0.0001
UniFrac distance (unweighted)	Year/Population	1	4	8.1	0.03	0.0002
	Community Age	9	8.2	16.5	0.61	0.0001
UniFrac distance (weighted)	Year/Population	1	6.8	5.7	0.04	0.0068
	Community Age	9	5.7	4.8	0.31	0.0001

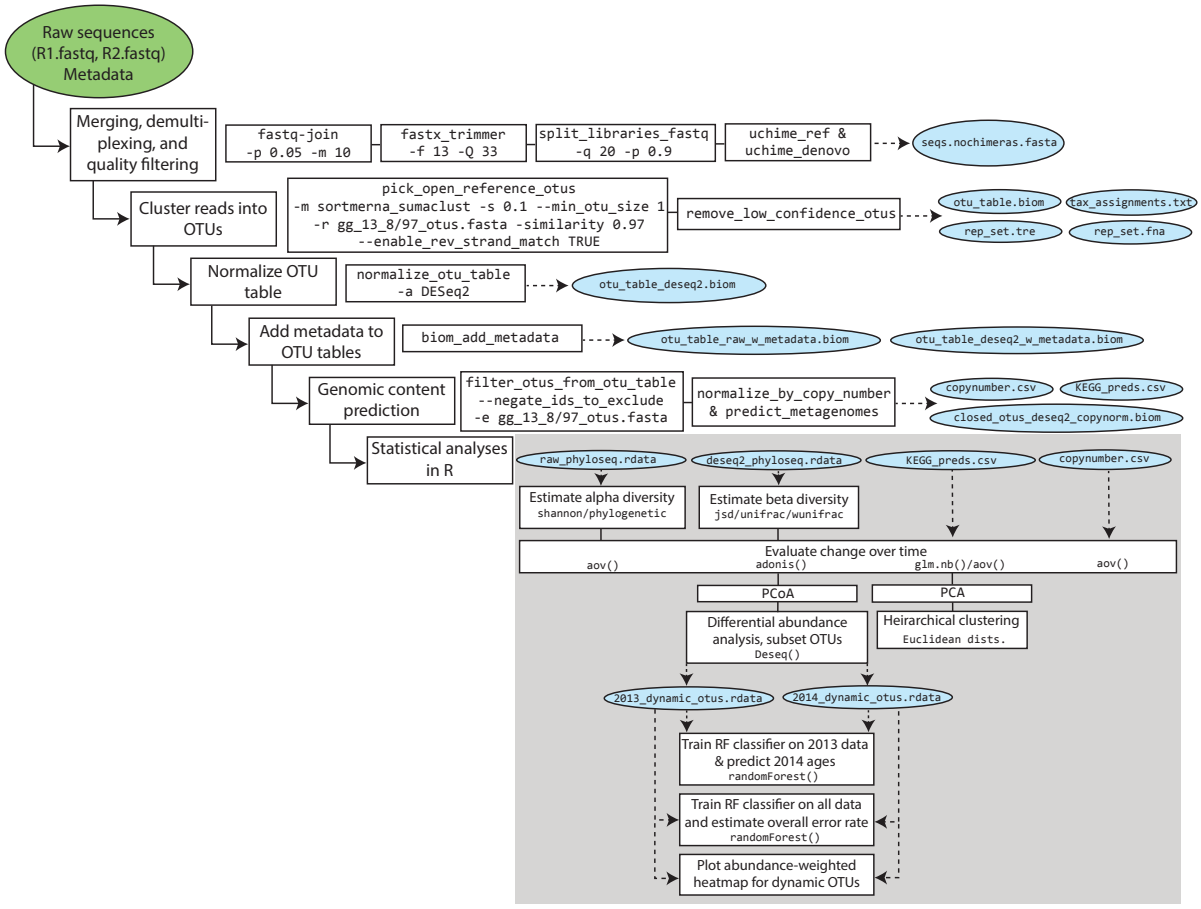

Figure S1. Bioinformatics workflow for 16S rRNA reads. Green circle denotes raw data, blue circles denote processed data files, leftmost boxes denote general steps applied to the data, and boxes to their right indicate specific computational or statistical steps. Grey box encompasses analytical steps performed using R.

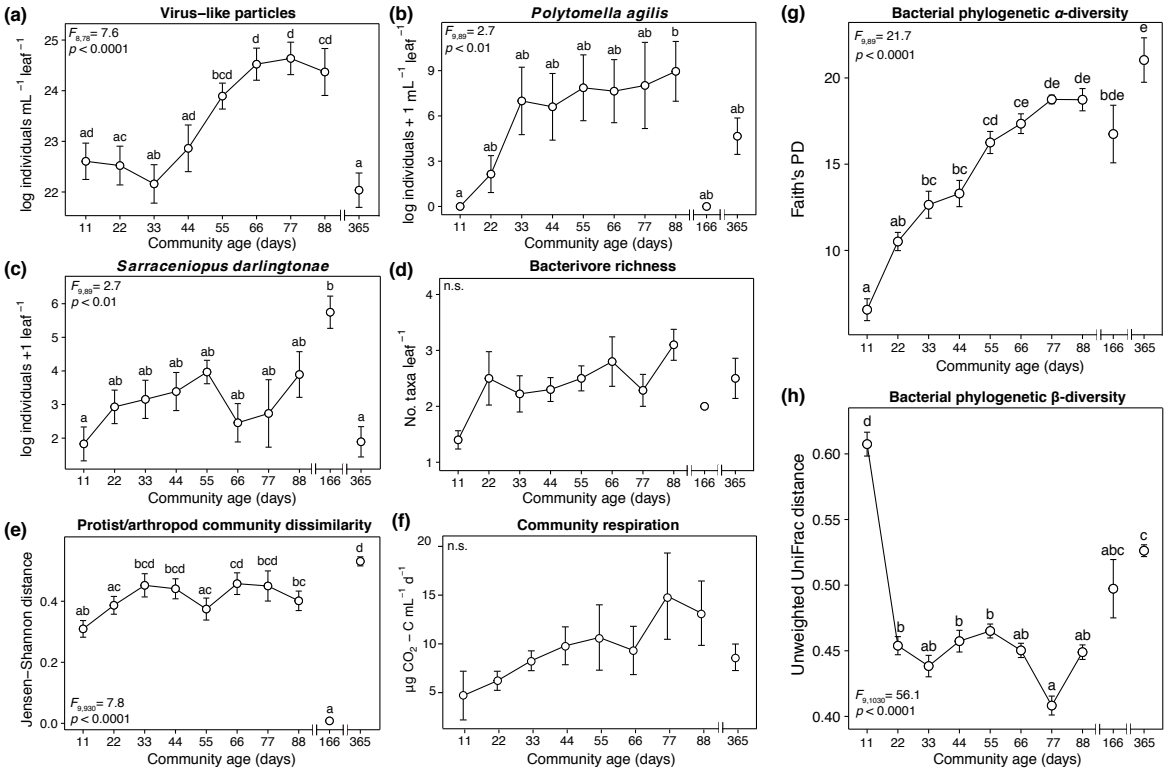

Figure S2. Successional trends in the abundances of **(a)** virus-like particles, **(b)** the flagellate *Polytomella agilis*, and **(c)** the mite *Sarraceniopus darlingtonae.* **(d)** Bacterivore (incl. flagellates, ciliates, mites, and rotifers) richness did not significantly change over the study period. **(e)** Beta diversity among bacterivore guilds did not significantly change until pitcher leaves diverged during year 2. **(f)** The respiration rates of communities placed in a common environment did not significantly change with age. Phylogenetic measures of bacterial **(g)** alpha and **(h)** beta diversities were qualitatively similar to OTU-based measures (see fig. 2 main text). Points denote mean values ± SEM.

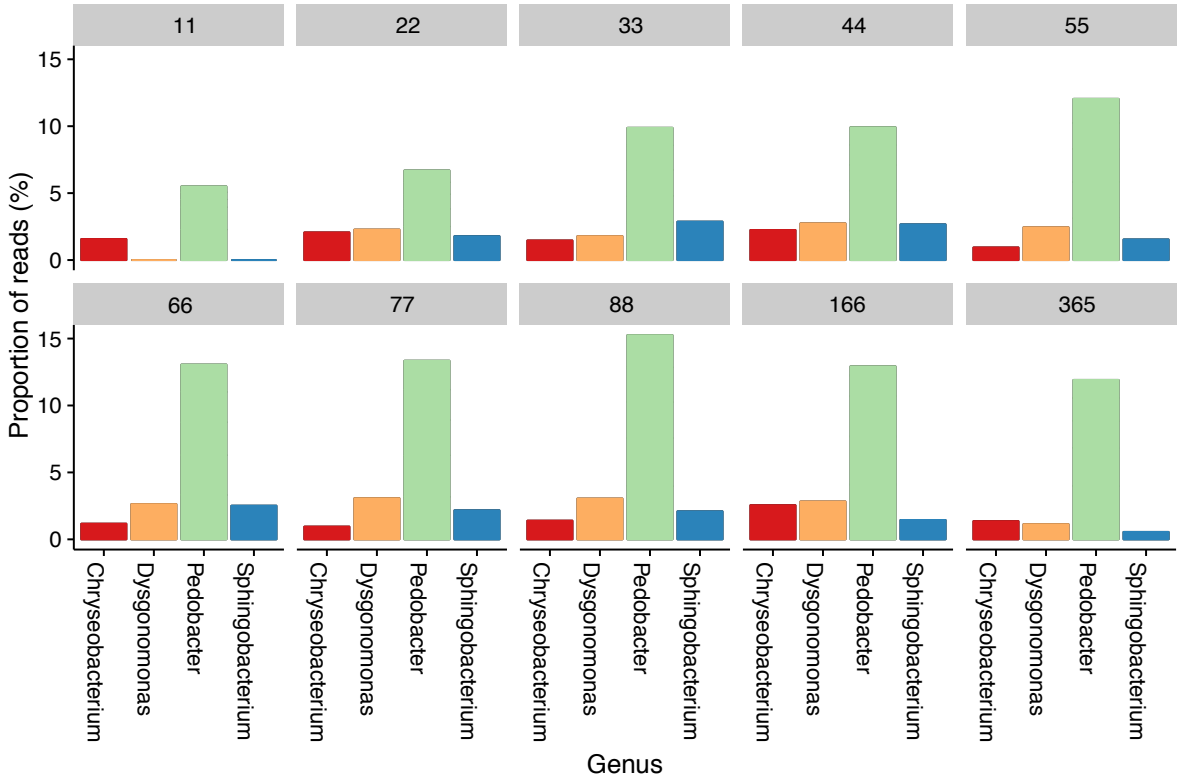

442

443 **Figure S3.** Trends in the most abundant OTUs (of the top 50) belonging to phylum

444 Bacteroidetes. Values denote the relative proportions of each genus compared to the rest of

445 the top 50 most abundant OTUs.

446

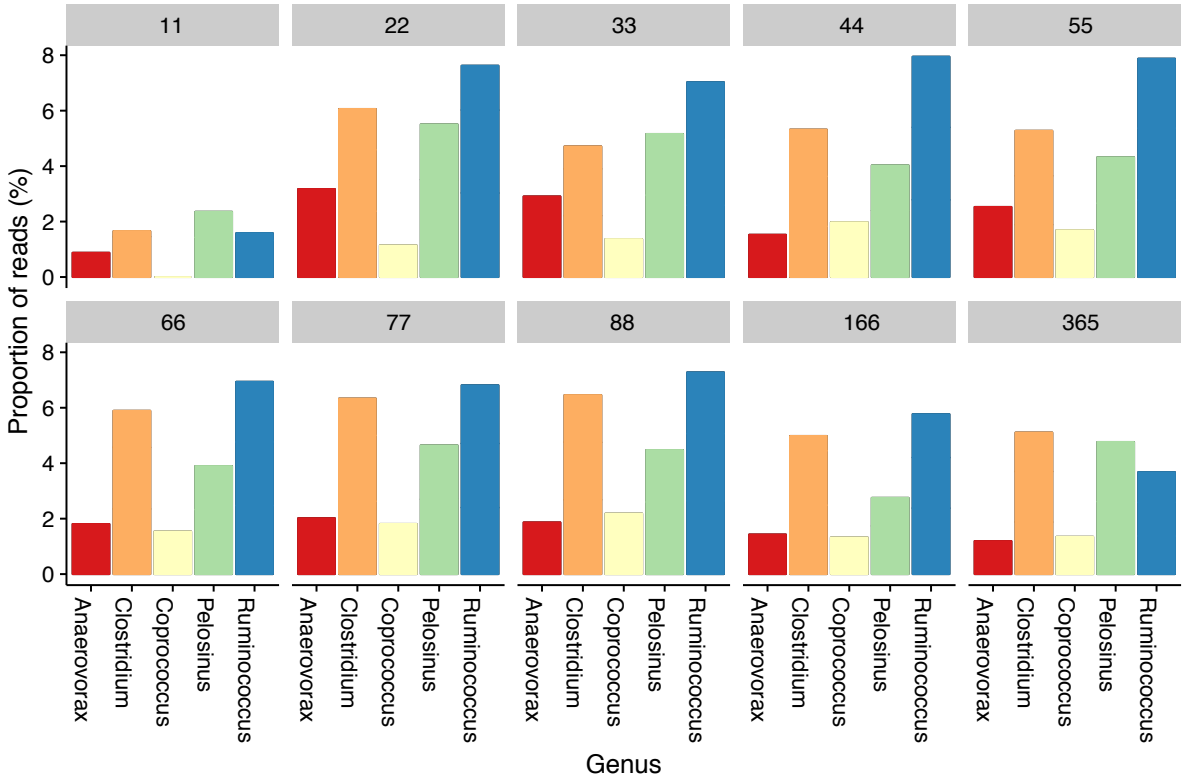

447

448 **Figure S4.** Trends in the top 50 most abundant OTUs (of the top 50) belonging to phylum

449 Firmicutes. Values denote the relative proportions of each genus compared to the rest of the

450 top 50 most abundant OTUs.

451

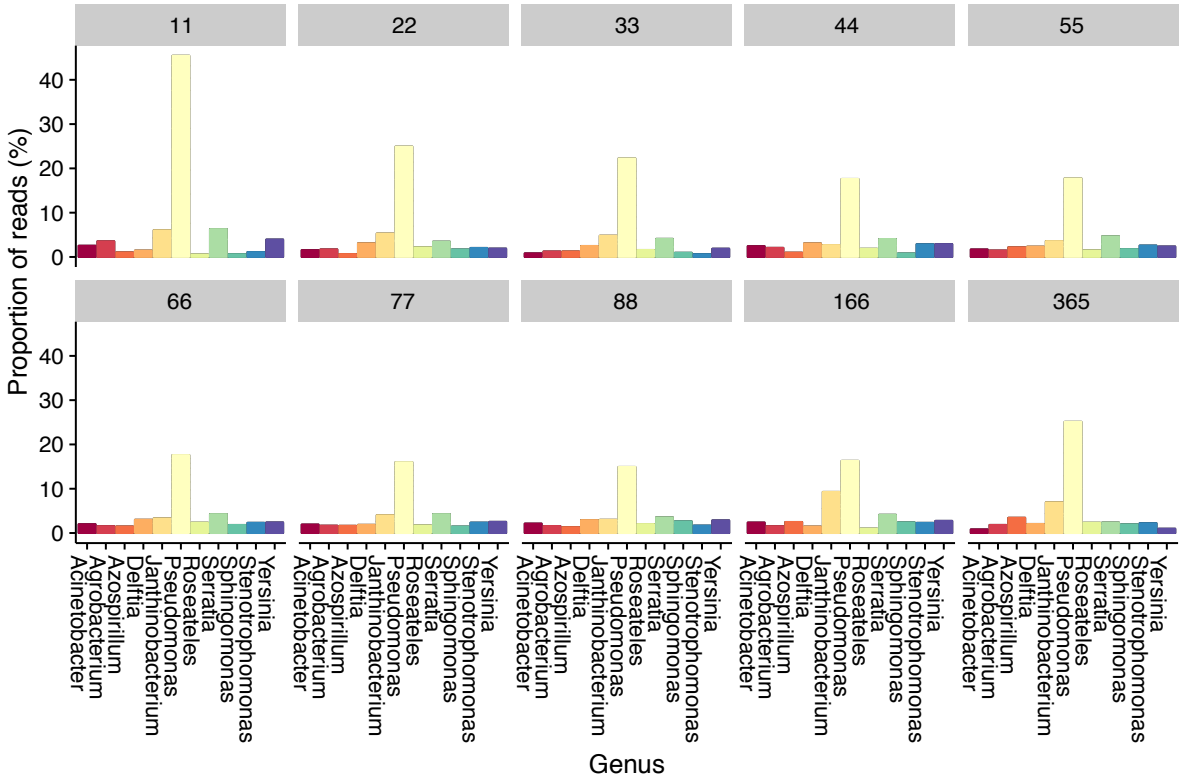

Figure S5. Trends in the top 50 most abundant OTUs (of the top 50) belonging to phylum Proteobacteria. Values denote the relative proportions of each genus compared to the rest of the top 50 most abundant OTUs.

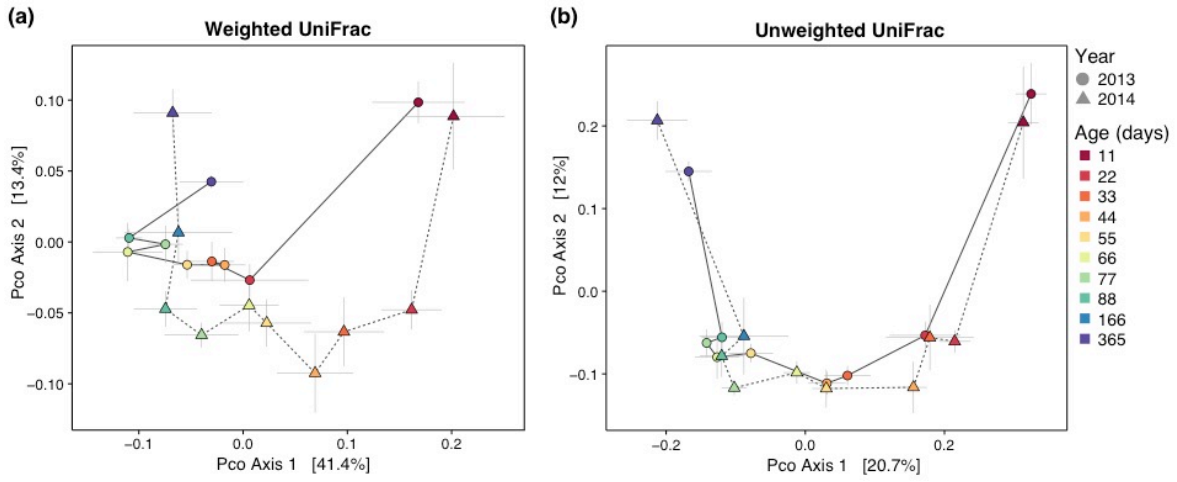

Figure S6. Principal coordinate (PCoA) plots for **(a)** weighted and **(b)** unweighted UniFrac distances between samples, demonstrating approximately parallel successional trajectories in bacterial community composition between years. The eigenvalue-based percentages of variance explained by the axes are displayed on each axis. Points denote centroids ± SEM.

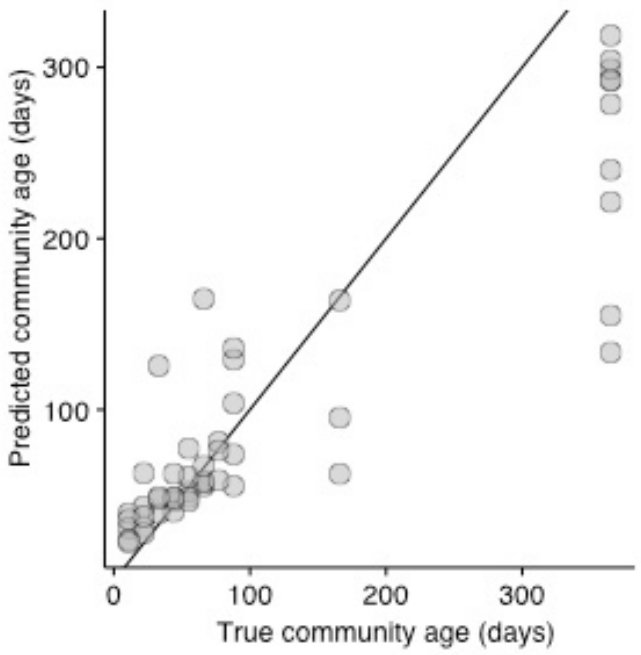

Figure S7. Observed versus predicted ages of 2014 pitchers classified using a random forest classifier trained on 2013 data ($R^2 = 0.75$). The solid line represents perfect 1:1 predictive accuracy.

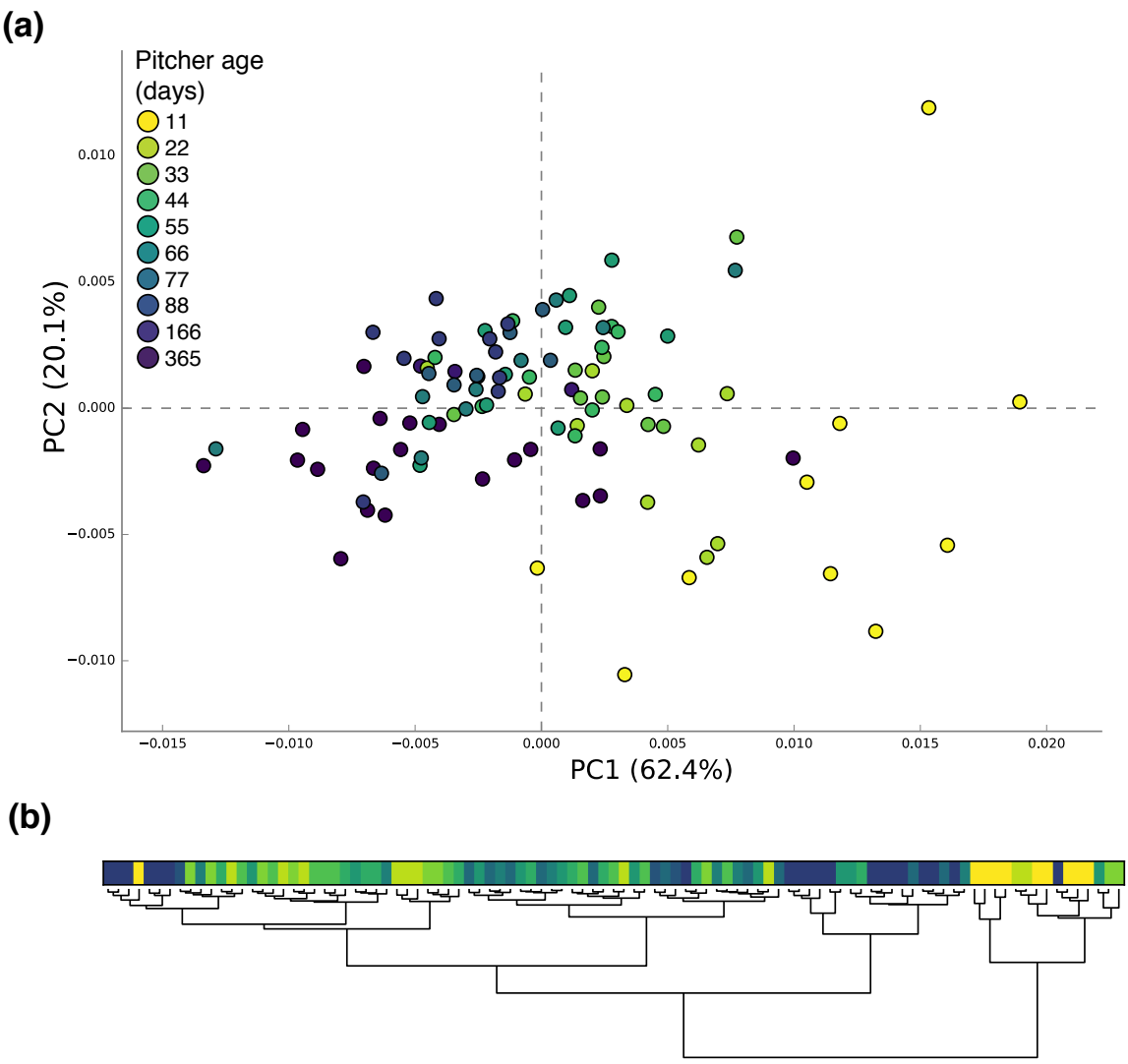

Figure S8. (a) Pitcher samples' PICRUSt-predicted metagenome contents generally separate by age along their first two principal component axes. **(b)** Hierarchical clustering results for these samples supports two major clades: one comprised of early (22-33 day) samples and the other comprised of middle- and late-stage samples.

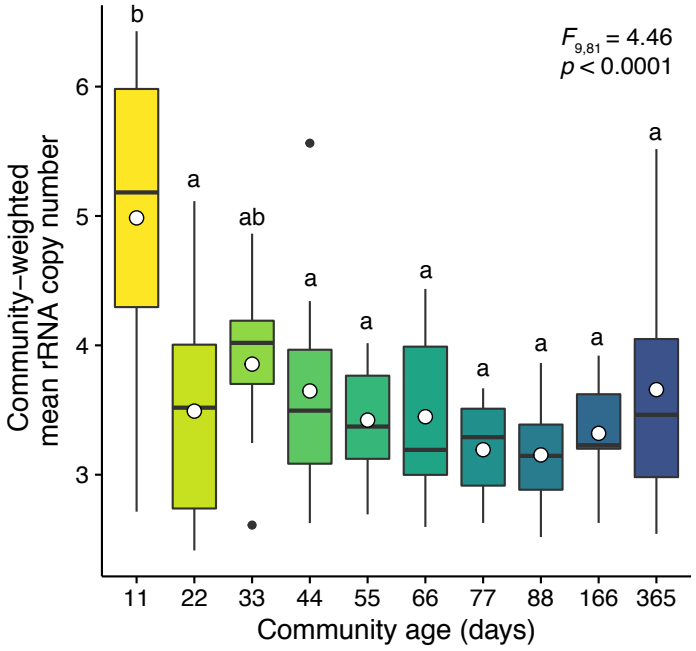

Figure S9. PICRUSt-predicted average rRNA copy numbers for OTUs in a sample. White points denote mean for each age class. Early-stage (11 day) pitcher communities contained OTUs with more rRNA copies than were predicted for later pitcher communities. Shared letters above groups indicate no significant post-hoc pairwise differences ($p > 0.05$).

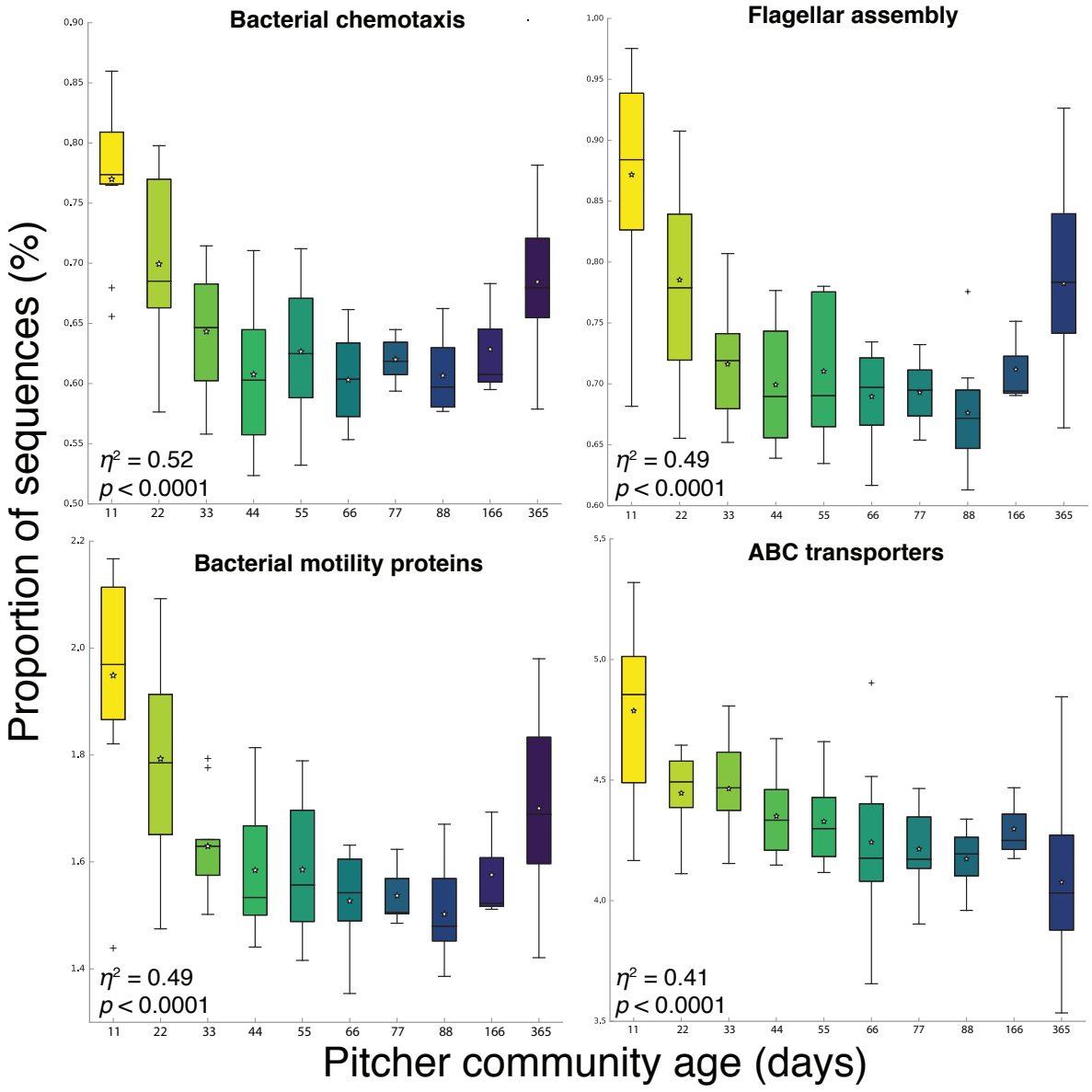

Figure S10. Patterns in the within-age class relative abundances of PICRUSt-predicted KEGG pathways. White points denote mean values for each age class. Pathways shown here are more abundant within young pitcher samples. P-values show the significant of age effects and η^2 values are a measure of age effect size.

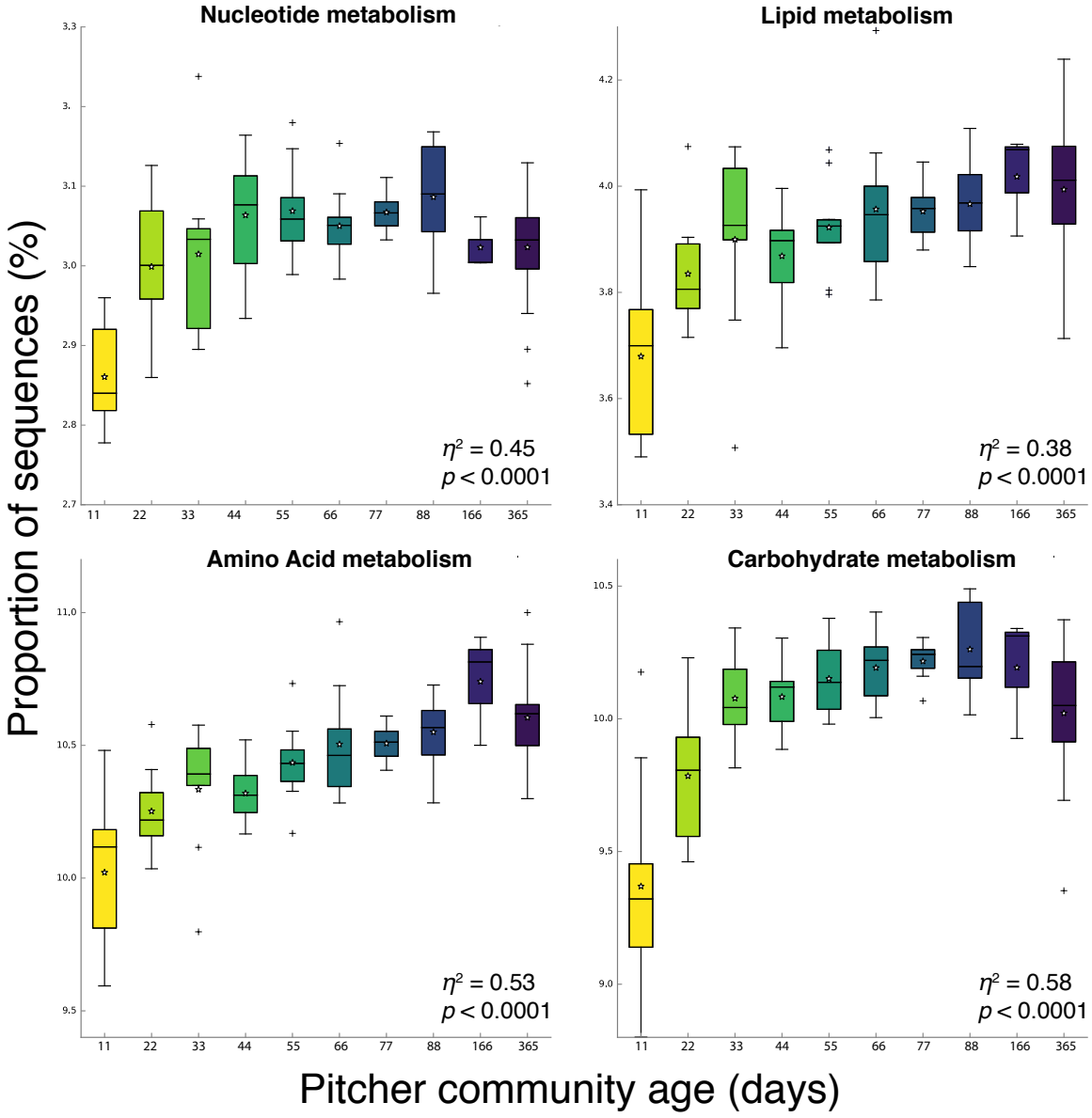

Figure S11. PICRUSt-predicted KEGG pathways for major metabolic pathways. Pathways shown here are more abundant within older pitcher samples. White points denote mean values for each age class. P-values show the significant of age effects and η^2 values are a measure of age effect size.

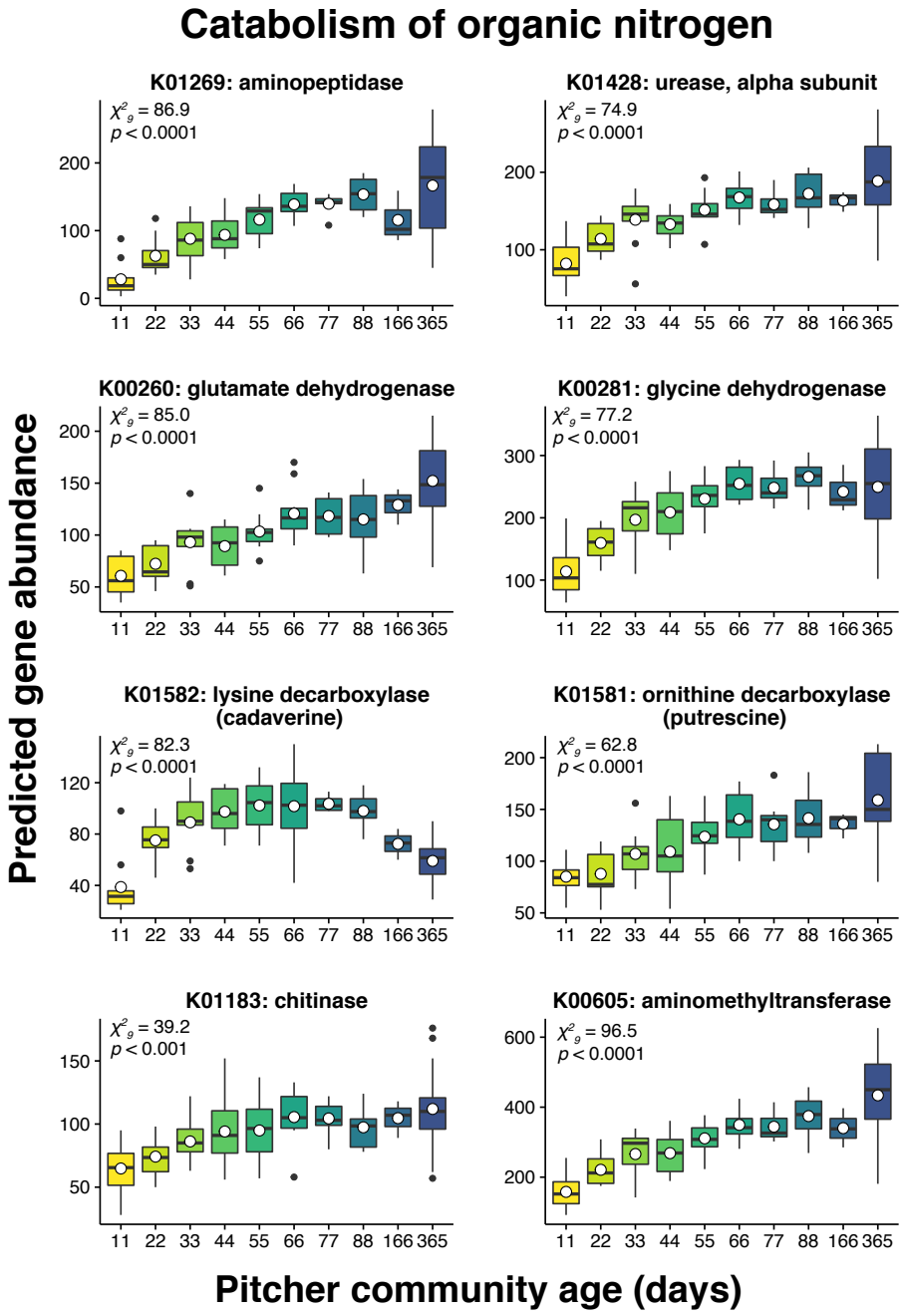

511

512 **Figure S12.** Temporal trends in the abundances of PICRUSt-predicted KEGG ortholog genes

513 involved in the catabolism and uptake of organic nitrogen and its conversion to ammonium.

514 White points denote mean values for each age class. χ^2 is the likelihood ratio test statistic for

515 the effect of pitcher age on gene abundance.

516

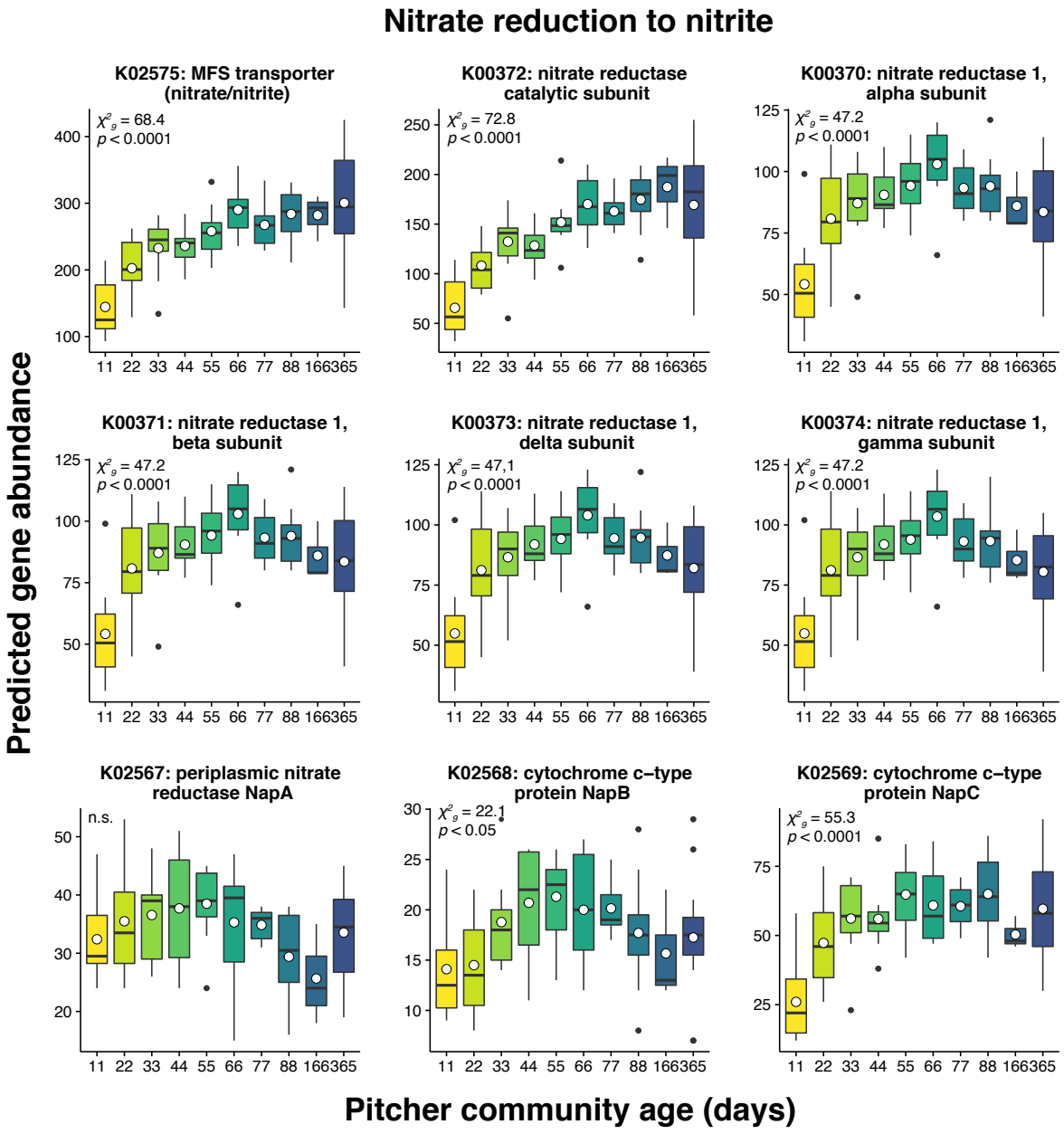

Figure S13. Temporal trends in the abundances of PICRUSt-predicted KEGG ortholog genes involved in the reduction of nitrate to nitrite. White points denote mean values for each age class. χ^2 is the likelihood ratio test statistic for the effect of pitcher age on gene abundance.

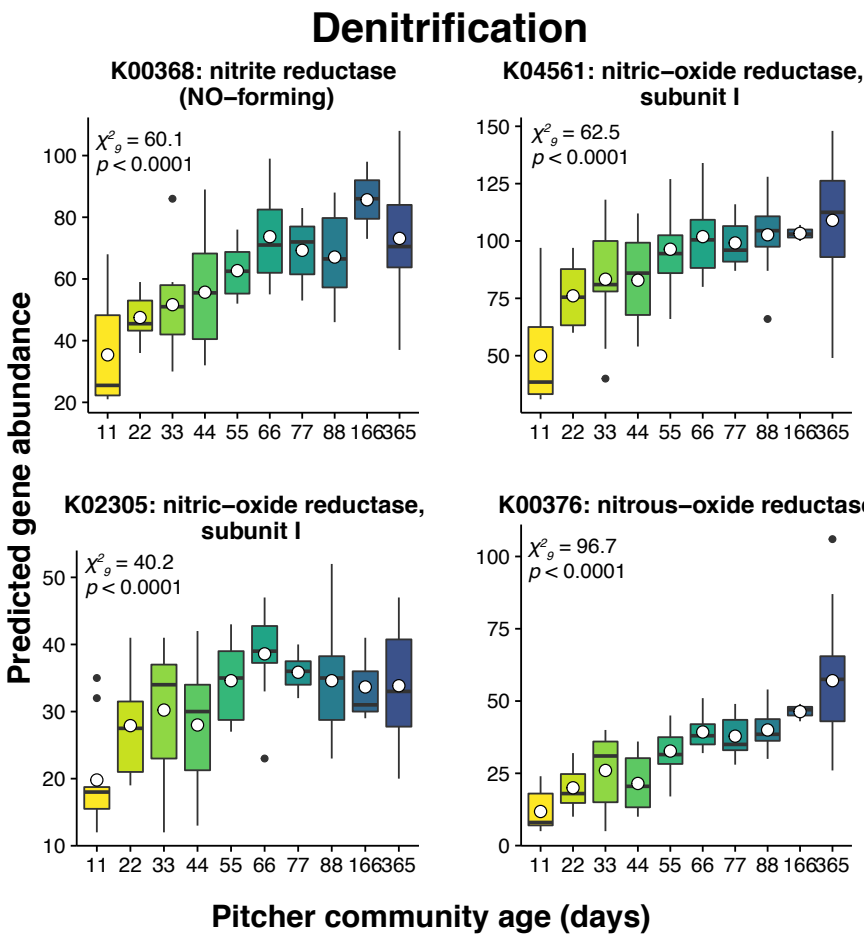

522

523 **Figure S14.** Temporal trends in the abundances of PICRUSt-predicted KEGG ortholog genes

524 involved in the conversion of nitrite to gaseous N_2. White points denote mean values for each

525 age class. χ^2 is the likelihood ratio test statistic for the effect of pitcher age on gene

526 abundance.

527

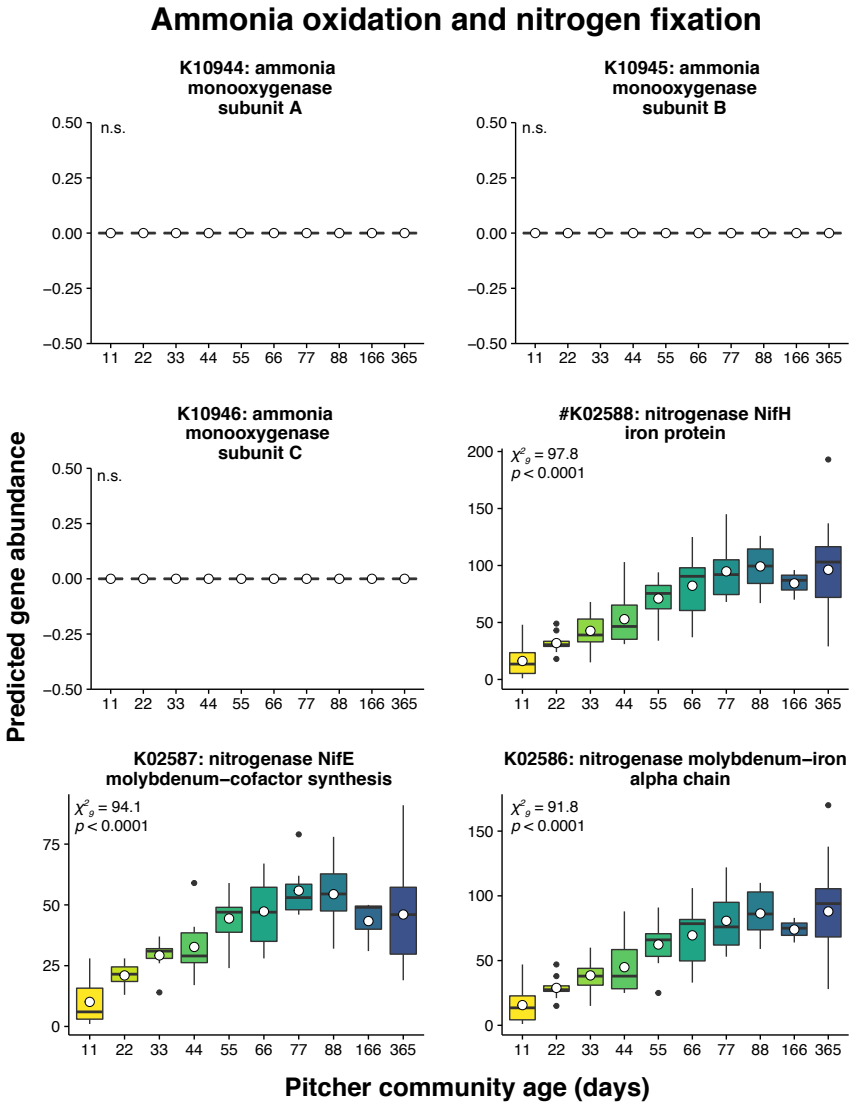

528

529 **Figure S15.** Temporal trends in the abundances of PICRUSt-predicted KEGG ortholog genes

530 involved in ammonia oxidation and nitrogen fixation. White points denote mean values for

531 each age class. χ^2 is the likelihood ratio test statistic for the effect of pitcher age on gene

532 abundance.

533

534